01 Jan 2008

Nonlinear H(Infinity) Missile Longitudinal Autopilot Design with Theta-D Method

Ming Xin

S. N. Balakrishnan
Missouri University of Science and Technology, bala@mst.edu

Recommended Citation

M. Xin and S. N. Balakrishnan, "Nonlinear H(Infinity) Missile Longitudinal Autopilot Design with Theta-D Method," *IEEE Transactions of Aerospace and Electronic Systems*, Institute of Electrical and Electronics Engineers (IEEE), Jan 2008.
The definitive version is available at https://doi.org/10.1109/TAES.2008.4516988

Nonlinear H_∞ Missile Longitudinal Autopilot Design with $\theta - D$ Method

M. XIN, Member, IEEE

S. N. BALAKRISHNAN
University of Missouri–Rolla

In this paper, a new nonlinear H_∞ control technique, called $\theta - D$ H_∞ method, is employed to design a missile longitudinal autopilot. The $\theta - D$ H_∞ design has the same structure as that of linear H_∞, except that the two Riccati equations that are part of the solution process are state dependent. The $\theta - D$ technique yields suboptimal solutions to nonlinear optimal control problems in the sense that it provides an approximate solution to the Hamilton-Jacobi-Bellman (HJB) equation. It is also shown that this method can be used to provide an approximate closed-form solution to the state dependent Riccati equation (SDRE) and consequently reduce the on-line computations associated with the nonlinear H_∞ implementation. A missile longitudinal autopilot design demonstrates the capabilities of $\theta - D$ method. This new nonlinear H_∞ design also shows favorable results as compared with the linear H_∞ design based on the linearized model.

Manuscript received May 10, 2004; revised May 28, 2005; released for publication January 16, 2007.

IEEE Log No. T-AES/44/1/920387.

Refereeing of this contribution was handled by Y. Oshman.

This work was supported by grants from the Naval Surface Warfare Center through Anteon Corporation.

Authors' addresses: S. N. Balakrishnan, Dept. of Mechanical and Aerospace Engineering, University of Missouri–Rolla, 1870 Miner Circle, Rolla, MO 65401, E-mail: (bala@umr.edu); M. Xin, Dept. of Aerospace Engineering, Mississippi State University, Jackson, MS 39762, E-mail: (xin@ae.msstate.edu).

I. INTRODUCTION

Missile autopilots are classically designed using linear control approaches such as frequency domain design, linear quadratic regulator or linear H_∞ robust control. The plant is linearized around fixed operating points. Gain scheduling [1–3] can then be used to cover the whole flight envelope. However, the dynamics of high performance aircrafts and missiles are inherently nonlinear due to inertial coupling, aerodynamic effects, and actuator limits. Though autopilot designs are typically based on linearized dynamics models, modern missile systems often operate in flight regimes where nonlinearities significantly affect the dynamic response. Many nonlinear control methods have been proposed for missile autopilot design in the past. Among the methods that have been investigated are nonlinear optimal and robust control design approaches based on the solutions to the Hamilton-Jacobi-Bellman (HJB) and Hamilton-Jacobi-Isaacs (HJI) equations, respectively. However solving these two partial differential equations analytically is very difficult. In [4], a power series expansion was used in the design of nonlinear flight control systems undergoing high angles of attack. This method was also applied to the control of highly maneuverable aircraft in [5] and compared with the performance of a conventional proportional-integral (PI) gain scheduled controller. The results showed similar performances. McLain and Beard [6] employed the successive Galerkin approximation technique to solve the HJB equation and applied it to the nonlinear missile autopilot design. But since the control laws are given as a series of basis functions, they are inherently complex to solve. In addition, to find an admissible control to satisfy all the ten conditions proposed here is not an easy task. Wise and Sedwick [7] employed nonlinear H_∞ optimal control to design a pitch plane autopilot for agile missiles. A control law was obtained by approximating the solution to the HJI equation using the classical method of characteristics. However, the design is still based on a gain scheduled linear H_∞ solution with the linearized dynamics. The nonlinearity is treated as a deviation from the linearized solution.

Another recently emerging technique that systematically solves the nonlinear regulator problem is the state dependent Riccati equation (SDRE) method [8]. By turning the equations of motion into a linear-like structure, this approach permits the designer to employ linear optimal control methods such as the linear quadratic regulator (LQR) methodology and the H_∞ design technique for the synthesis of nonlinear control systems. It can be used for a broad class of nonlinear regulator problems [9]. In [10], a state dependent Riccati differential equation approach was used to design an integrated missile guidance and control. The problem was formulated as a nonlinear H_∞

control problem. As stated in this paper, the SDRE approach is computationally intensive and, thus, requires significant processor capability for on-line implementation. The reason is that the SDRE method needs on-line computation of the algebraic Riccati equation at **each sample time** when implemented. The method developed in this study yields approximate analytical solutions.

In this paper, a new suboptimal nonlinear controller synthesis ($\theta - D$ approximation) technique based on an approximate solution to the HJB equation is proposed. By introducing an intermediate variable θ and perturbations to the cost function, the HJB equation is reduced to a set of recursive algebraic equations. Solving these equations successively gives a closed-form expression for suboptimal control. In [11], the $\theta - D$ H_2 formulation was used to design a nonlinear missile longitudinal autopilot to track normal accelerations. This approach has also been successfully employed to design a six degree-of-freedom nonlinear hybrid bank-to-turn/skid-to-turn missile autopilot in [12].

In [8], the SDRE H_∞ problem was formulated and shown to lead to solving two SDREs for a feedback control. However, solving two Riccati equations on-line is very time consuming. In this paper, the $\theta - D$ H_∞ design is proposed to address the same problem as in [13]. We demonstrate that the $\theta - D$ H_∞ design does not require on-line solutions of Riccati equation and gives an approximate closed-form solution to the two SDREs associated with the nonlinear H_∞ problem. We also compare the linear H_∞ control results based on the linearized dynamics with our nonlinear H_∞ design and show that the linear design is not able to produce good tracking response in the face of large state variations.

The rest of the paper is organized as follows. The nonlinear missile longitudinal dynamics are described in Section II. In Section III, the $\theta - D$ H_∞ formulation is presented; design of the missile autopilot with this technique is developed in Section IV. Numerical results and analysis are given in Section V. Conclusions are made in Section VI.

II. NONLINEAR MISSILE LONGITUDINAL DYNAMICS

The missile model used here is taken from [13]. The model assumes constant mass, i.e., post burnout, no roll rate, zero roll angle, no sideslip, and no yaw rate. The nonlinear equations of motion for a rigid airframe reduce to two force equations, one moment equation, and one kinematic equation

$$\dot{U} + qW = \frac{\sum F_{B_X}}{m} \tag{1}$$

$$\dot{W} - qU = \frac{\sum F_{B_Z}}{m} \tag{2}$$

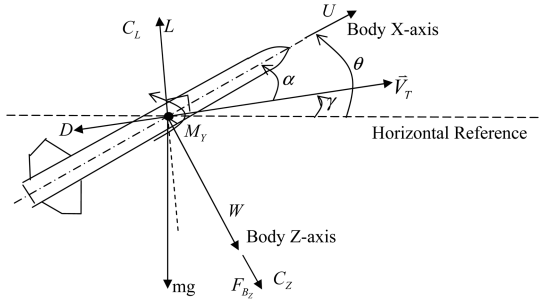

Fig. 1. Longitudinal forces and moment acting on missile.

$$\dot{q} = \frac{\sum M_Y}{I_Y} \tag{3}$$

$$\dot{\theta} = q \tag{4}$$

where U and W are components of velocity vector $\vec{V}_T$ along the body-fixed X and Z axes; θ is the pitch angle; q is the pitch rate about the body Y axis; m is the missile mass. The forces along the body-fixed coordinates and moments about the center of gravity are shown in Fig. 1.

The forces and moment about the center of gravity are described by

$$\sum F_{B_X} = L\sin\alpha - D\cos\alpha - mg\sin\theta \tag{5}$$

$$\sum F_{B_Z} = -L\cos\alpha - D\sin\alpha + mg\cos\theta \tag{6}$$

$$\sum M_Y = \bar{M} \tag{7}$$

where α is the angle of attack, L denotes aerodynamic lift, D denotes drag, and $\bar{M}$ is the total pitching moment. The lift, drag, and pitching moment are as follows

$$L = \tfrac{1}{2}\rho V_T^2 S C_L, \qquad D = \tfrac{1}{2}\rho V_T^2 S C_D, \qquad \bar{M} = \tfrac{1}{2}\rho V_T^2 S d C_m \tag{8}$$

where ρ is the air density and V_T is the missile speed, i.e., $V_T = \sqrt{U^2 + W^2}$. Note that the normal force coefficient is used to calculate the lift and drag coefficients:

$$C_L = -C_Z\cos\alpha, \qquad C_D = C_{D_0} - C_Z\sin\alpha \tag{9}$$

where C_{D_0} is the drag coefficient at zero angle of attack.

The nondimensional aerodynamic coefficients for the missile at 20,000 ft altitude are [13]:

$$C_Z = a_n\alpha^3 + b_n\alpha|\alpha| + c_n\left(2 - \frac{M}{3}\right)\alpha + d_n\delta \tag{10}$$

$$C_m = a_m\alpha^3 + b_m\alpha|\alpha| + c_m\left(-7 + \frac{8M}{3}\right)\alpha + d_m\delta + e_m q. \tag{11}$$

In this paper, we adopt Mach number M, angle of attack α, flight path angle γ, and pitch rate q as the

TABLE I
Aerodynamic Coefficients

Force	Moment
$a_n = 19.373$	$a_m = 40.440$
$b_n = -31.023$	$b_m = -64.015$
$c_n = -9.717$	$c_m = 2.922$
$d_n = -1.948$	$d_m = -11.803$
$C_{D_0} = 0.300$	$e_m = -1.719$

TABLE II
Physical Parameters

Symbol	Name	Value
P_0	Static Pressure	973.3 lb/ft^2
I_Y	Moment of Inertia	182.5 slug – ft^2
S	Reference Area	0.44 ft^2
d	Reference Length	0.75 ft
m	Mass	13.98 slug
a	Speed of Sound	1036.4 ft/s
g	Gravity	32.2 ft/s^2

elements of the state space since they appear in the expressions for the aerodynamic coefficients. Note that

$$\tan\alpha = \frac{W}{U}, \qquad V_T = U^2 + W^2$$
$$M = \frac{V_T}{a}, \qquad \gamma = \theta - \alpha \tag{12}$$

and

$$\dot{M} = \frac{\dot{V}_T}{a}, \qquad \dot{V}_T = \frac{\dot{U}U + \dot{W}W}{V_T}. \tag{13}$$

The state equations of motion can now be written as

$$\dot{M} = \frac{0.7P_0S}{ma}[M^2(C_{D_0} - C_Z\sin\alpha)] - \frac{g}{a}\sin\gamma \tag{14}$$

$$\dot{\alpha} = \frac{0.7P_0S}{ma}MC_Z\cos\alpha + \frac{g}{aM}\cos\gamma + q \tag{15}$$

$$\dot{\gamma} = -\frac{0.7P_0S}{ma}MC_Z\cos\alpha - \frac{g}{aM}\cos\gamma \tag{16}$$

$$\dot{q} = \frac{0.7P_0Sd}{I_Y}M^2C_m. \tag{17}$$

Numerical values for the coefficients in (10) and (11) are given in Table I and the physical parameters associated with this missile are given in Table II.

Substitution of the parameter values into (14)–(17) yields:

$$\dot{M} = 0.4008M^2\alpha^3\sin\alpha - 0.6419M^2|\alpha|\alpha\sin\alpha - 0.2010M^2\left(2 - \frac{M}{3}\right)\alpha\sin\alpha - 0.0062M^2 - 0.0403M^2\sin\alpha\delta - 0.0311\sin\gamma \tag{18}$$

$$\dot{\alpha} = 0.4008M\alpha^3\cos\alpha - 0.6419M|\alpha|\alpha\cos\alpha - 0.2010M\left(2 - \frac{M}{3}\right)\alpha\cos\alpha - 0.0403M\cos\alpha\delta - 0.0311\frac{\cos\gamma}{M} + q \tag{19}$$

$$\dot{\gamma} = -0.4008M\alpha^3\cos\alpha + 0.6419M|\alpha|\alpha\cos\alpha + 0.2010M\left(2 - \frac{M}{3}\right)\alpha\cos\alpha + 0.0403M\cos\alpha\delta + 0.0311\frac{\cos\gamma}{M} \tag{20}$$

$$\dot{q} = 49.82M^2\alpha^3 - 78.86M^2|\alpha|\alpha + 3.60M^2\left(-7 + \frac{8M}{3}\right)\alpha - 14.54M^2\delta - 2.12M^2q. \tag{21}$$

A second-order actuator dynamics is included in the design and analysis. This model is given by

$$\begin{bmatrix}\dot{\delta}\\ \ddot{\delta}\end{bmatrix} = \begin{bmatrix}0 & 1\\ -\omega_a^2 & -2\zeta\omega_a\end{bmatrix}\begin{bmatrix}\delta\\ \dot{\delta}\end{bmatrix} + \begin{bmatrix}0\\ \omega_a^2\end{bmatrix}\delta_c \tag{22}$$

where the damping ratio $\varsigma = 0.7$, and the natural frequency $\omega_a = 50$.

III. FORMULATION OF THE NONLINEAR H_∞ PROBLEM

Consider a general nonlinear system

$$\dot{x} = f(x) + B_w(x)w + B_u(x)u \tag{23}$$

$$z = c_z(x) + D_{zu}(x)u \tag{24}$$

$$y = c_y(x) + D_{yw}(x)w \tag{25}$$

where $x \in R^n$, $u \in R^{m_1}$, $w \in R^{m_2}$, w is the exogenous input including tracking command and noises injected into the system, $\mathbf{u}$ is the control, $\mathbf{z}$ is the performance output, and y is the measurement output. Assume that all these functions are smooth and $\mathbf{f(0) = 0}$. It is desired to find a controller such that the closed-loop system is internally stable and for $\gamma \geq 0$

$$\int_0^T \|z(t)\|^2dt \leq \gamma^2\int_0^T \|w(t)\|^2dt \tag{26}$$

for all $T \geq 0$ and all $w \in L_2(0,T)$. Then the exogenous signals will be attenuated by γ. The $\theta - D$ H_∞ formulation is a natural extension of the linear H_∞ design. Bring the nonlinear dynamics to the linear-like structure

$$\dot{x} = A(x)x + B_w(x)w + B_u(x)u \tag{27}$$

$$z = C_z(x)x + D_{zu}(x)u \tag{28}$$

$$y = C_y(x)x + D_{yw}(x)w \tag{29}$$

such that $[A(x), B_w(x)]$, $[A(x), B_u(x)]$ and $[C_z(x), A(x)]$, $[C_y(x), A(x)]$ are pointwise stabilizable and detectable,

respectively, for $x \in \Omega$, where Ω is a compact set in R^n.

If the coefficient matrices $A(x)$, $B_w(x)$, $B_u(x)$, $C_z(x)$, $D_{zu}(x)$, $C_y(x)$, $D_{yw}(x)$ are constant matrices, the standard linear H_∞ problem leads to solving the two Riccati equations given below in terms of their Hamiltonians [14]

$$H_1: \quad \begin{bmatrix} A - B_u R_u^{-1} R_{12}^T & \gamma^{-2} B_w B_w^T - B_u R_u^{-1} B_u^T \\ -R_1 + R_{12} R_u^{-1} R_{12}^T & -(A - B_u R_u^{-1} R_{12}^T)^T \end{bmatrix} \tag{30}$$

$$H_2: \quad \begin{bmatrix} (A - V_{12} R_w^{-1} C_y)^T & \gamma^{-2} C_z^T C_z - C_y^T R_w^{-1} C_y \\ -V_1 + V_{12} R_w^{-1} V_{12}^T & -(A - V_{12} R_w^{-1} C_y) \end{bmatrix} \tag{31}$$

where

$$\begin{aligned} V_1 &= B_w B_w^T, \qquad V_{12} = B_w D_{yw}^T \\ R_w &= D_{yw} D_{yw}^T \qquad R_1 = C_z^T C_z \\ R_{12} &= C_z^T D_{zu} \qquad \text{and} \qquad R_u = D_{zu}^T D_{zu}. \end{aligned} \tag{32}$$

The nonlinear H_∞ formulation we are proposing is a natural extension of the linear H_∞ formulation in the sense that the matrices in Hamiltonians H_1 and H_2 are state dependent. For later use, we assume that (30) and (31) are state dependent and we omit the **x** for brevity. Assume that the solution to the SDREs (30) and (31) are **X** and **Y**, respectively.

Also, the nonlinear feedback controller is constructed via

$$\frac{d\hat{x}}{dt} = A_c(\hat{x})\hat{x} + B_c(\hat{x})y \tag{33}$$

$$u = F(\hat{x})\hat{x} \tag{34}$$

where A_c, B_c, and F are

$$A_c = A + B_u F + \gamma^{-2} B_w B_w^T X + ZL(C_y + \gamma^{-2} D_{yw} B_w^T X) \tag{35}$$

$$B_c = -ZL, \qquad Z = (I - \gamma^{-2} YX)^{-1} \tag{36}$$

$$F = -R_u^{-1}[B_u^T X + R_{12}^T], \qquad L = -(YC_y^T + B_w D_{yw}^T) R_w^{-1}. \tag{37}$$

γ has to be sufficiently large such that the following three conditions are satisfied [9]

(i) $X(\hat{x}) > 0$ (ii) $Y(\hat{x}) > 0$ and

(iii) $\rho[X(\hat{x})Y(\hat{x})] < \gamma^2$

where ρ represents the maximum eigenvalue. Up to this point, this is the same formulation as the SDRE H_∞ [9]. However, to employ the SDRE H_∞ controller, one needs to solve the algebraic Riccati equations (30) and (31) on-line at each sample point.

IV. SOLUTION TO THE NONLINEAR H_∞ PROBLEM USING $\theta - D$ METHOD

The $\theta - D$ suboptimal control technique [15] can be used to find an approximate closed-form solution to the SDRE-like equations (30) and (31). The basic procedure of applying the $\theta - D$ method is summarized as follows [15].

The class of nonlinear time-invariant systems that the $\theta - D$ method is addressing is described by

$$\dot{x} = f(x) + B(x)u. \tag{38}$$

The objective is to find a controller that minimizes the quadratic cost function:

$$J = \frac{1}{2}\int_0^\infty (x^T Q x + u^T R u) dt \tag{39}$$

where $x \in \Omega \subset R^n$, $f \in R^n$, $B \in R^{n\times m}$, $u \in U \subset R^m$, $Q \in R^{n\times n}$, $R \in R^{m\times m}$, Q is a semi-positive definite constant matrix, and **R** is a positive definite constant matrix. It is assumed that Ω and U are compact sets in R^n and R^m, respectively, and that $f(x)$ is continuously differentiable in **x** on Ω and $\mathbf{f(0) = 0}$.

The solution to the infinite-horizon nonlinear optimal control problem represented by (38), (39) can be obtained by solving the HJB partial differential equation [16]:

$$\frac{\partial V^T}{\partial x} f(x) - \frac{1}{2}\frac{\partial V^T}{\partial x} B(x) R^{-1} B^T(x) \frac{\partial V}{\partial x} + \frac{1}{2} x^T Q x = 0 \tag{40}$$

where $V(0) = 0$, $V(x) > 0$, and $V(x)$ is continuously differentiable.

The expression for optimal control is given by

$$u = -R^{-1} B^T(x) \frac{\partial V}{\partial x} \tag{41}$$

and the optimal cost is obtained by using (41) as

$$V(x) = \min_u \frac{1}{2}\int_t^\infty (x^T Q x + u^T R u) dt. \tag{42}$$

Since a closed-form solution to $\partial V/\partial x$ is difficult to obtain, the $\theta - D$ method is used to find approximate solutions to the HJB equation. To this end, perturbations are added to the cost function which transfers equation (39) to

$$J = \frac{1}{2}\int_0^\infty \left\{ x^T \left[Q + \sum_{i=1}^\infty D_i \theta^i \right] x + u^T R u \right\} dt \tag{43}$$

where θ is an intermediate variable used for the purpose of power series expansion. θ and D_i are chosen such that $Q + \sum_{i=1}^\infty D_i \theta^i$ is semi-positive definite.

For later use, we rewrite the state equation as

$$\begin{aligned} \dot{x} &= f(x) + B(x)u \\ &= \left\{ A_0 + \theta \left[\frac{A(x)}{\theta} \right] \right\} x + \left\{ g_0 + \theta \left[\frac{g(x)}{\theta} \right] \right\} u \end{aligned} \tag{44}$$

where $\mathbf{A}_0$ is chosen to be a constant matrix such that (A_0, g_0) is a stabilizable pair and $\{[A_0 + A(x)], [g_0 + g(x)]\}$ is pointwise controllable. The resulting perturbed HJB equation corresponding to (43) becomes

$$\frac{\partial V^T}{\partial x} f(x) - \frac{1}{2}\frac{\partial V^T}{\partial x} B(x) R^{-1} B^T(x) \frac{\partial V}{\partial x} + \frac{1}{2} x^T \left(Q + \sum_{i=1}^{\infty} D_i \theta^i \right) x = 0. \tag{45}$$

Define

$$\lambda = \frac{\partial V}{\partial x}. \tag{46}$$

Then, a power series solution to λ is assumed to be

$$\lambda = \frac{\partial V}{\partial x} = \sum_{i=0}^{\infty} T_i \theta^i x \tag{47}$$

where T_i are assumed to be symmetric matrix. Now, the problem reduces to determination of T_i.

A recursive $\theta - D$ algorithm to calculate T_i is obtained by substituting (47) into the HJB equation (45) and equating the coefficients of powers of θ to zero:

$$T_0 A_0 + A_0^T T_0 - T_0 g_0 R^{-1} g_0^T T_0 + Q = 0 \tag{48}$$

$$T_1(A_0 - g_0 R^{-1} g_0^T T_0) + (A_0^T - T_0 g_0 R^{-1} g_0^T) T_1 = -\frac{T_0 A(x)}{\theta} - \frac{A^T(x) T_0}{\theta} + T_0 g_0 R^{-1} \frac{g^T(x)}{\theta} T_0 + T_0 \frac{g(x)}{\theta} R^{-1} g_0^T T_0 - D_1 \tag{49}$$

$$T_2(A_0 - g_0 R^{-1} g_0^T T_0) + (A_0^T - T_0 g_0 R^{-1} g_0^T) T_2 = -\frac{T_1 A(x)}{\theta} - \frac{A^T(x) T_1}{\theta} + T_0 g_0 R^{-1} \frac{g^T(x)}{\theta} T_1 + T_0 \frac{g(x)}{\theta} R^{-1} g_0^T T_1 + T_0 \frac{g(x)}{\theta} R^{-1} \frac{g^T(x)}{\theta} T_0 + T_1 g_0 R^{-1} g_0^T T_1 + T_1 g_0 R^{-1} \frac{g^T(x)}{\theta} T_0 + T_1 \frac{g(x)}{\theta} R^{-1} g_0^T T_0 - D_2 \tag{50}$$

$$T_n(A_0 - g_0 R^{-1} g_0^T T_0) + (A_0^T - T_0 g_0 R^{-1} g_0^T) T_n = -\frac{T_{n-1} A(x)}{\theta} - \frac{A^T(x) T_{n-1}}{\theta} + \sum_{j=0}^{n-2} T_j \frac{g(x)}{\theta} R^{-1} \frac{g^T(x)}{\theta} T_{n-2-j} + \sum_{j=0}^{n-1} T_j \left[g_0 R^{-1} \frac{g^T(x)}{\theta} + \frac{g(x)}{\theta} R^{-1} g_0^T \right] T_{n-1-j} + \sum_{j=1}^{n-1} T_j g_0 R^{-1} g_0^T T_{n-j} - D_n. \tag{51}$$

As the right-hand side of (49)–(51) is a function of $\mathbf{x}$ and θ, we denote T_i as $T_i(x, \theta)$ accordingly. Note that (48) is an algebraic Riccati equation and that equations (49)–(51) are Lyapunov equations that are linear in terms of $T_i(x, \theta)$. The resulting feedback control can be written as

$$u = -R^{-1} B^T(x) \frac{\partial V}{\partial x} = -R^{-1} B^T(x) \sum_{i=0}^{\infty} T_i(x, \theta) \theta^i x. \tag{52}$$

The key component of the $\theta - D$ approach is the perturbation matrices D_i, $i = 1, \ldots n$ constructed in the following pattern:

$$D_1 = k_1 e^{-l_1 t} \left[-\frac{T_0 A(x)}{\theta} - \frac{A^T(x) T_0}{\theta} + T_0 g_0 R^{-1} \frac{g^T(x)}{\theta} T_0 + T_0 \frac{g(x)}{\theta} R^{-1} g_0^T T_0 \right] \tag{53}$$

$$D_2 = k_2 e^{-l_2 t} \left[-\frac{T_1 A(x)}{\theta} - \frac{A^T(x) T_1}{\theta} + T_0 g_0 R^{-1} \frac{g^T(x)}{\theta} T_1 + T_0 \frac{g(x)}{\theta} R^{-1} g_0^T T_1 + T_0 \frac{g(x)}{\theta} R^{-1} \frac{g^T(x)}{\theta} T_0 + T_1 g_0 R^{-1} \frac{g^T(x)}{\theta} T_0 + T_1 \frac{g(x)}{\theta} R^{-1} g_0^T T_0 + T_1 g_0 R^{-1} g_0^T T_1 \right] \tag{54}$$

$$\vdots$$

$$D_n = k_n e^{-l_n t} \left\{ -\frac{T_{n-1} A(x)}{\theta} - \frac{A^T(x) T_{n-1}}{\theta} + \sum_{j=0}^{n-1} T_j \left[g_0 R^{-1} \frac{g^T(x)}{\theta} + \frac{g(x)}{\theta} R^{-1} g_0^T \right] T_{n-1-j} + \sum_{j=0}^{n-2} T_j \frac{g(x)}{\theta} R^{-1} \frac{g^T(x)}{\theta} T_{n-2-j} + \sum_{j=1}^{n-1} T_j g_0 R^{-1} g_0^T T_{n-j} \right\} \tag{55}$$

where k_i and $l_i > 0$, $i = 1, \ldots n$ are design parameters.

The justification of constructing D_i in this manner stems from the fact that large values for initial control may be introduced by the $\theta - D$ algorithm when initial states are large if there are no D_i terms on the right-hand side of (49)–(51). This is due to the state dependent terms $A(x)$ and $g(x)$ that could grow to a high magnitude as $\mathbf{x}$ is large. For example, when $A(x)$ includes a cubic term, its magnitude could be large if $\mathbf{x}$ is large. This large value will be reflected in the solution for T_i, i.e., the left-hand side of (49)–(51) as the Lyapunov equation is linear and has a

constant coefficient. Due to the recursive nature of the algorithm, this large value will be further propagated into the solution for T_{i+1} and amplified to even higher values. Ultimately it could lead to higher levels of control or even instability. So if D_i is chosen such that

$$
\begin{aligned}
&-\frac{T_{i-1}A(x)}{\theta}-\frac{A^T(x)T_{i-1}}{\theta}+\sum_{j=0}^{i-2}T_j\frac{g(x)}{\theta}R^{-1}\frac{g^T(x)}{\theta}T_{i-2-j}\\
&+\sum_{j=0}^{i-1}T_j\left(g_0R^{-1}\frac{g^T(x)}{\theta}+\frac{g(x)}{\theta}R^{-1}g_0^T\right)T_{i-1-j}\\
&+\sum_{j=1}^{i-1}T_jg_0R^{-1}g_0^TT_{i-j}-D_i\\
&\quad=\varepsilon_i(t)\left\{-\frac{T_{i-1}A(x)}{\theta}-\frac{A^T(x)T_{i-1}}{\theta}\right.\\
&\qquad+\sum_{j=0}^{i-1}T_j\left[g_0R^{-1}\frac{g^T(x)}{\theta}+\frac{g(x)}{\theta}R^{-1}g_0^T\right]T_{i-1-j}\\
&\qquad+\sum_{j=0}^{i-2}T_j\frac{g(x)}{\theta}R^{-1}\frac{g^T(x)}{\theta}T_{i-2-j}\\
&\qquad\left.+\sum_{j=1}^{i-1}T_jg_0R^{-1}g_0^TT_{i-j}\right\} \qquad (56)
\end{aligned}
$$

where

$$\varepsilon_i(t)=1-k_ie^{-l_it} \qquad (57)$$

is a small number, ε_i can be used to suppress this large value from propagating in (49)–(51). In summary, there are three functions for ε_i. The first usage is to suppress the large control from occurring. The second function is to satisfy some conditions required in the proof of convergence and stability of the above algorithm [15]. The third usage is to modulate the system transient performance by adjusting the parameters of k_i and l_i. On the other hand, the exponential term e^{-l_it} with $l_i>0$ is used to make the perturbation terms in the cost function and HJB equation die out very quickly.

REMARK θ is just an intermediate variable. The introduction of θ is for the convenience of power series expansion. It turns out to be cancelled when we multiply θ^i in the final control calculation, i.e., (52).

The $\theta-D$ method can be summarized in the following steps:

1) The first algebraic Riccati equation (48) is solved to get T_0 once A_0, g_0, $\mathbf{Q}$, and $\mathbf{R}$ are determined. Note that the resulting T_0 is a positive definite constant matrix.

2) Solve the Lyapunov equation (49) to get $T_1(x,\theta)$. An interesting property of this as well as the rest of equations is that the coefficient matrices $A_0-g_0R^{-1}g_0^TT_0$ and $A_0^T-T_0g_0R^{-1}g_0^T$ are constant matrices. Let $A_{c_0}=A_0-g_0R^{-1}g_0^TT_0$. Through linear algebra, (49) can be brought into a form like $\hat{A}_0\mathrm{Vec}(T_1)=\mathrm{Vec}[Q_1(x,\theta,t)]$ where $Q_1(x,\theta,t)$ is the right-hand side of (49); $\mathrm{Vec}(M)$ denotes stacking the elements of matrix $\mathbf{M}$ by rows in a column vector form; $\hat{A}_0=I\otimes A_{c_0}^T+A_{c_0}^T\otimes I$ is a constant matrix and the symbol $\otimes$ denotes the Kronecker product. The resulting solution of T_1 can be written as a closed-form expression $\mathrm{Vec}(T_1)=\hat{A}_0^{-1}\mathrm{Vec}[Q_1(x,\theta,t)]$.

3) Solve (50)–(51) by following the procedure in step 2. The number of T_is needed depends on the applications. Simulation results show that T_0, T_1, and T_2 are sufficient to achieve satisfactory performance for this missile autopilot problem.

As can be seen, closed-form solutions for $T_1,\ldots,T_n$ can be obtained with just one matrix inverse operation. The expression of $Q_i(x,\theta,t)$ on the right-hand side of the equations is already known and needs simple matrix multiplications and additions.

From the above procedure we can observe that the $\theta-D$ method gives an approximate closed-form solution to the HJB equation if we take a finite number of terms in the expression for control. Next we show that this approach in fact also gives an approximate solution to the SDRE.

The first step to show relationship between the SDRE and $\theta-D$ methods is to assume that $P(x)=\sum_{i=0}^{\infty}T_i(x,\theta)\theta^i$. As seen from (46) and (47),

$$\frac{\partial V}{\partial x}=P(x)x. \qquad (58)$$

Also write $f(x)$ in (38) as a state dependent coefficient form:

$$f(x)=\bar{A}(x)x. \qquad (59)$$

Substituting (58) and (59) into the HJB equation (40) we can obtain the SDRE:

$$\bar{A}^T(x)P(x)+P(x)\bar{A}(x)-P(x)B(x)R^{-1}B^T(x)P(x)+Q=0. \qquad (60)$$

Therefore the $\theta-D$ approach gives an approximate closed-form solution to this SDRE (60) if we take a finite number of terms of T_i. To be more specific, in the nonlinear H_∞ formulation, the two Hamiltonians (30) and (31) can be related to (60) respectively as follows.

For Hamiltonian (30):

$$
\begin{aligned}
A-B_uR_u^{-1}R_{12}^T&=\bar{A}(x)\\
B_uR_u^{-1}B_u^T-\gamma^{-2}B_wB_w^T&=B(x)R^{-1}B(x) \qquad (61)\\
R_1-R_{12}R_u^{-1}R_{12}^T&=Q.
\end{aligned}
$$

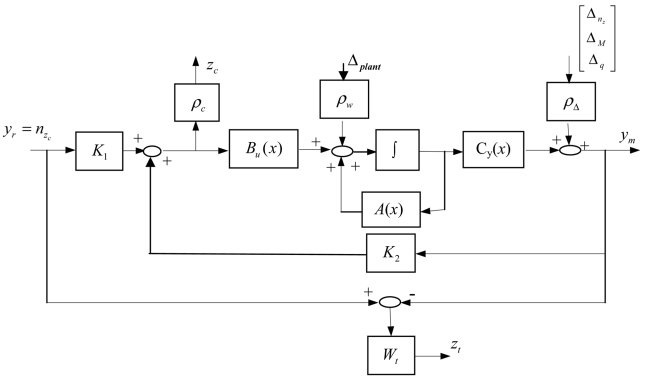

Fig. 2. Tracking block diagram.

For Hamiltonian (31):

$$[A - V_{12}R_w^{-1}C_y]^T = \bar{A}(x)$$
$$C_y^T R_w^{-1} C_y - \gamma^{-2} C_z^T C_z = B(x)R^{-1}B(x) \tag{62}$$
$$V_1 - V_{12}R_w^{-1}V_{12}^T = Q.$$

In the next section, the $\theta - D$ approach is used to solve the nonlinear H_∞ problem by solving the two state dependent Hamiltonian (30) and (31).

V. MISSILE LONGITUDINAL AUTOPILOT DESIGN

The controller objective is to design a suboptimal controller which is able to drive the system to track the commanded normal acceleration (in g) in the presence of process noise and measurement noise. The tracking block diagram is shown in Fig. 2.

The Kalman gain K_1 and K_2 are the solutions of the dynamic feedback controller (33)–(34). The control weight is ρ_c, the plant disturbance weight is ρ_w, and the output disturbance weight is ρ_Δ. The performance weighting function for tracking error: $n_{Z_c} - n_Z$:

$$W_t(s) = \frac{1}{s + 0.001} \tag{63}$$

or in a state space form:

$$W_t = \left[\begin{array}{c|c} A_t & B_t \\ \hline C_t & 0 \end{array}\right] = \begin{bmatrix} -0.001 & 1 \\ 1 & 0 \end{bmatrix}. \tag{64}$$

The performance output is

$$z = [z_t \quad z_c]^T \tag{65}$$

where z_t is the weighted tracking error and z_c is the weighted control output.

The states for the design and simulation are chosen to be

$$x = [M, \alpha, \gamma, q, \delta, \dot{\delta}, x_t]^T \tag{66}$$

where x_t is the state associated with the weighting function W_t.

The control variable is the fin deflection:

$$u = \delta_c. \tag{67}$$

The measurement vector is

$$y_m = [n_z \quad M \quad q]^T \tag{68}$$

where n_z is the normal acceleration (in gs) which is described by the equation:

$$n_z = \frac{\sum F_{B_Z}}{mg} + \cos\theta = \frac{0.7P_0S}{mg}M^2C_Z + \cos(\gamma + \alpha). \tag{69}$$

In terms of the flight conditions at 20,000 ft altitude n_z is

$$n_z = 12.901M^2\alpha^3 - 20.659M^2|\alpha|\alpha - 6.471M^2\left(2 - \frac{M}{3}\right)\alpha - 1.297M^2\delta + \cos(\gamma + \alpha). \tag{70}$$

The acceleration command

$$y_r = n_{z_c}. \tag{71}$$

So the output vector in the controller design is

$$y = [y_r \quad y_m]^T = [n_{z_c} \quad y_m]^T = [n_{z_c} \quad n_z \quad M \quad q]^T. \tag{72}$$

The exogenous input w consists of the commanded normal acceleration n_{z_c}, process noise Δ_{plant}, and measurement noise Δ_{nz}, Δ_M, and Δ_q which are associated with the measured normal acceleration, Mach number, and pitch rate, respectively, i.e.,

$$w = [n_{z_c} \quad \Delta_{\text{plant}} \quad \Delta_{n_z} \quad \Delta_M \quad \Delta_q]^T. \tag{73}$$

In the simulation, they are assumed Gaussian with unit variance.

The plant noise weights are chosen to be

$$\rho_w = [0.2 \quad 0.01 \quad 0.01 \quad 0.2 \quad 0.01 \quad 0.01]^T. \tag{74}$$

The measurement noise weights on n_z, M, and q are, respectively, the diagonal elements of

$$\rho_\Delta = \begin{bmatrix} 0.01 & 0 & 0 \\ 0 & 0.001 & 0 \\ 0 & 0 & 0.01 \end{bmatrix}. \tag{75}$$

The noise weights are chosen to be the same as the variance of the random number generator used in the simulation. The control weight ρ_c is used as the design parameter which appears in D_{zu} matrix in (28).

The state dependent coefficient matrix $A(x)$ and $C_y(x)$ in (27) and (29) are given in (76) and (77):

$$A(x)=\begin{bmatrix} -0.0062M & \begin{matrix}0.4008M^2\alpha^2\sin\alpha-0.6419M^2|\alpha|\sin\alpha\\ -0.2010M^2\left(2-\frac{M}{3}\right)\sin\alpha\end{matrix} & -0.0311\frac{\sin\gamma}{\gamma} & 0 & -0.0403M^2\sin\alpha & 0 & 0\\ -0.0311\frac{\cos\gamma}{M^2} & \begin{matrix}0.4008M\alpha^2\cos\alpha-0.6419M|\alpha|\cos\alpha\\ -0.2010M\left(2-\frac{M}{3}\right)\cos\alpha\end{matrix} & 0 & 1 & -0.0403M\cos\alpha & 0 & 0\\ 0.0311\frac{\cos\gamma}{M^2} & \begin{matrix}-0.4008M\alpha^2\cos\alpha+0.6419M|\alpha|\cos\alpha\\ +0.2010M\left(2-\frac{M}{3}\right)\cos\alpha\end{matrix} & 0 & 0 & 0.0403M\cos\alpha & 0 & 0\\ 0 & 49.82M^2\alpha^2-78.86M^2|\alpha|+3.6M^2\left(-7+\frac{8M}{3}\right) & 0 & -2.12M^2 & -14.54M^2 & 0 & 0\\ 0 & 0 & 0 & 0 & 0 & 1 & 0\\ 0 & 0 & 0 & 0 & -2500 & -70 & 0\\ -\frac{\cos(\gamma+\alpha)}{M} & -12.901M^2\alpha^2+20.659M^2|\alpha|+6.471M^2\left(2-\frac{M}{3}\right) & 0 & 0 & 1.297M^2 & 0 & A_t \end{bmatrix} \tag{76}$$

$$C_y(x)=\begin{bmatrix} 0 & 0 & 0 & 0 & 0 & 0 & 0\\ \frac{\cos(\gamma+\alpha)}{M} & 12.901M^2\alpha^2-20.659M^2|\alpha|-6.471M^2\left(2-\frac{M}{3}\right) & 0 & 0 & 1.297M^2 & 0 & 0\\ 1 & 0 & 0 & 0 & 0 & 0 & 0\\ 0 & 0 & 0 & 1 & 0 & 0 & 0 \end{bmatrix}. \tag{77}$$

The other coefficient matrices in state space (27)–(29) are given by

$$B_w=\begin{bmatrix} 0_{6\times1} & \rho_w & 0_{6\times1} & 0_{6\times2}\\ B_t & 0 & B_t\rho_{\Delta_{n_z}} & 0_{1\times2}\end{bmatrix}$$

$$B_u=[0\quad 0\quad 0\quad 0\quad 0\quad \omega_a^2\quad 0]^T$$

$$C_z=\begin{bmatrix} 0_{1\times6} & C_t\\ 0_{1\times6} & 0\end{bmatrix}$$

$$D_{zu}=\begin{bmatrix}0\\ \rho_c\end{bmatrix}$$

$$D_{yw}=\begin{bmatrix} 1 & 0 & 0_{1\times3}\\ 0_{3\times1} & 0_{3\times1} & \rho_\Delta\end{bmatrix}$$

where $\rho_{\Delta_{n_z}}$ is the measurement noise weight on n_z that is 0.01.

In order to avoid numerical problems during the simulation, in (76), $\sin\gamma/\gamma$ is set to 1 when γ is less than 10^{-4}.

The factorization of nonlinear equation (44) is as follows:

$$\dot{x}=\left\{\bar{A}(x_0)+\theta\left[\frac{\bar{A}(x)-\bar{A}(x_0)}{\theta}\right]\right\}x+\left\{B(x_0)+\theta\left[\frac{B(x)-B(x_0)}{\theta}\right]\right\}u \tag{78}$$

with $\bar{A}(x)$ defined by (61) and (62). The advantage of choosing this factorization is that in the $\theta-D$ formulation T_0 is solved from A_0 and g_0. If we select $A_0=\bar{A}(x_0)$ and $g_0=B(x_0)$, we have a good starting point for T_0 because $\bar{A}(x_0)$ and $B(x_0)$ retain much more system information than an arbitrary choice of A_0 and g_0.

VI. NUMERICAL RESULTS AND ANALYSIS

The simulation scenario is to initially command zero g then at 1 s start a square wave normal acceleration command of 10 gs returning to zero at 3 s. The initial conditions for the simulation were: Mach number 2.5 with the rest of variables being 0. The simulation was run at 100 samples per second. In solving the two SDREs (30) and (31) with the $\theta-D$ method, we used T_0, T_1, and T_2 in (52). Three terms have been found to be a good enough approximation in this problem. More terms could be added if needed. The $\theta-D$ design parameters were chosen as

$$D_1=e^{-10t}\left[-\frac{T_0\bar{A}(x)}{\theta}-\frac{\bar{A}^T(x)T_0}{\theta}+T_0g_0R^{-1}\frac{g^T(x)}{\theta}T_0+T_0\frac{g(x)}{\theta}R^{-1}g_0^TT_0\right] \tag{79}$$

$$D_2=e^{-10t}\left[-\frac{T_1\bar{A}(x)}{\theta}-\frac{\bar{A}^T(x)T_1}{\theta}+T_0g_0R^{-1}\frac{g^T(x)}{\theta}T_1+T_0\frac{g(x)}{\theta}R^{-1}g_0^TT_1+T_0\frac{g(x)}{\theta}R^{-1}\frac{g^T(x)}{\theta}T_0+T_1g_0R^{-1}\frac{g^T(x)}{\theta}T_0+T_1\frac{g(x)}{\theta}R^{-1}g_0^TT_0+T_1g_0R^{-1}g_0^TT_1\right]. \tag{80}$$

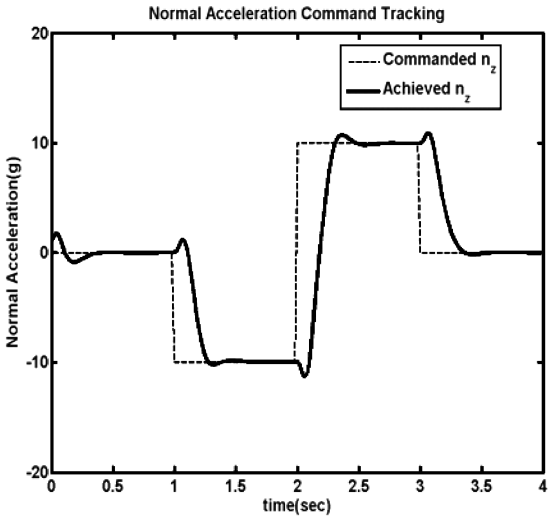

Fig. 3. Normal acceleration with $\rho_c = 1.3$, $\gamma = 4$.

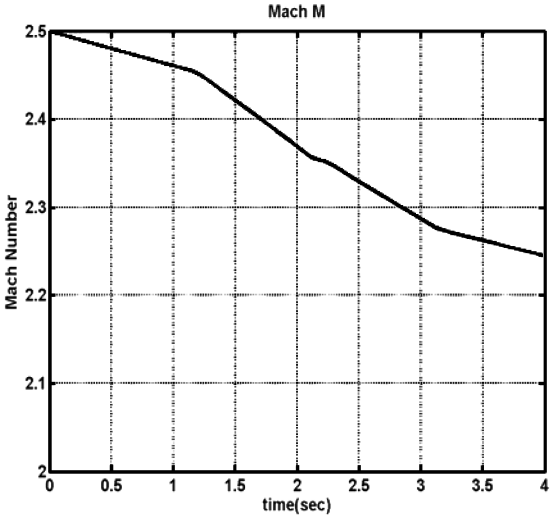

Fig. 5. Mach number response with $\rho_c = 1.3$, $\gamma = 4$.

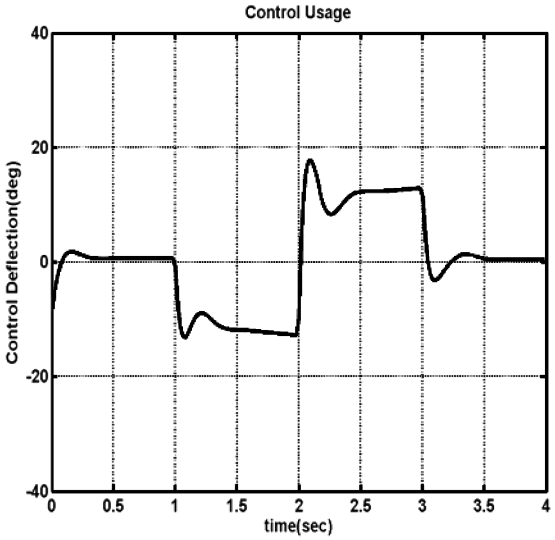

Fig. 4. Control usage with $\rho_c = 1.3$, $\gamma = 4$.

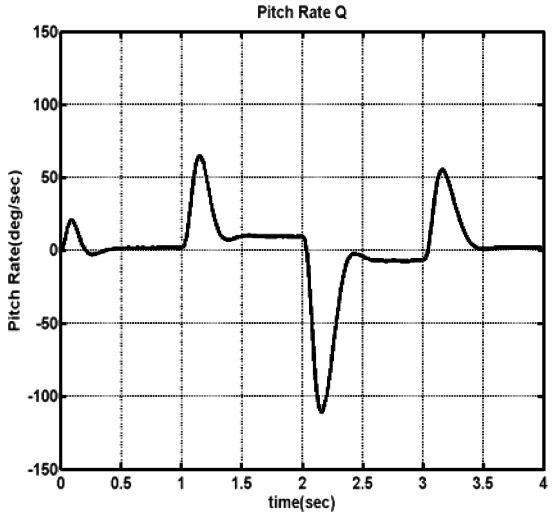

Fig. 6. Pitch rate response with $\rho_c = 1.3$, $\gamma = 4$.

The control weight ρ_c is set to 1.3. Figs. 3–9 demonstrate the results when γ is set to 4. The process of seeking γ is started with a large enough value for the constant γ to make sure the three conditions for the existence of the H_∞ solution, i.e., $X(\hat{x}) > 0$, $Y(\hat{x}) > 0$ and $\rho[X(\hat{x})Y(\hat{x})] < \gamma^2$ are satisfied. Systematically, the value of γ is reduced until one of these conditions is violated. Setting a constant γ is for the purpose of estimating a lower bound of γ that can be used as a starting point for seeking a varying value of γ as the feedback control is calculated at each instant. In doing so, the on-line iteration time is reduced. As can be seen in Fig. 3, the achieved normal acceleration tracks the command very well. The control trajectory and state responses are all well behaved which are shown in Figs. 4–8. Fig. 9 shows that $\rho[X(\hat{x})Y(\hat{x})]$ is less than γ^2. We present the plot of $\rho[X(\hat{x})Y(\hat{x})]$ because usually the condition of $\rho[X(\hat{x})Y(\hat{x})] < \gamma^2$ is most likely to fail before the other two conditions, i.e., $X(\hat{x}) > 0$ and

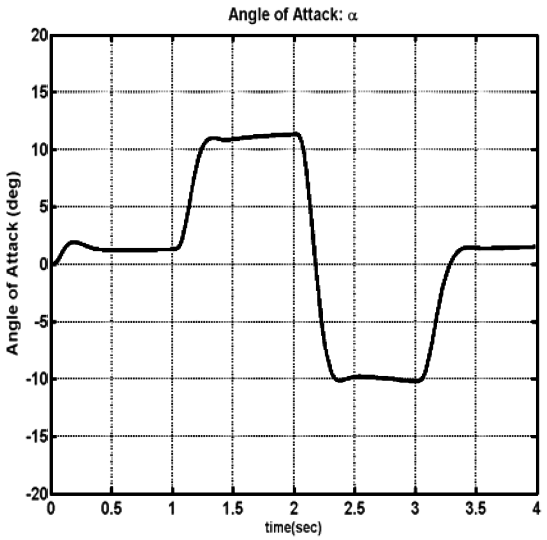

Fig. 7. Angle of attack response with $\rho_c = 1.3$, $\gamma = 4$.

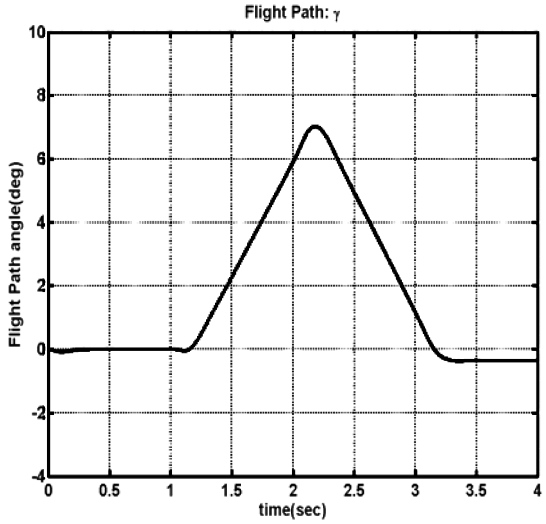

Fig. 8. Flight path angle response with $\rho_c = 1.3$, $\gamma = 4$.

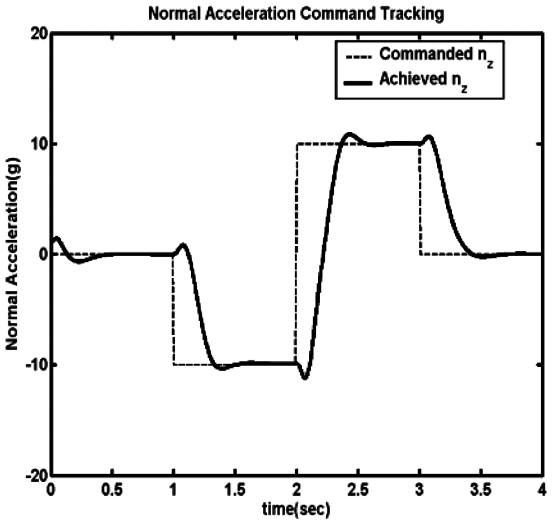

Fig. 10. Normal acceleration with $\rho_c = 2$, $\gamma = 4$.

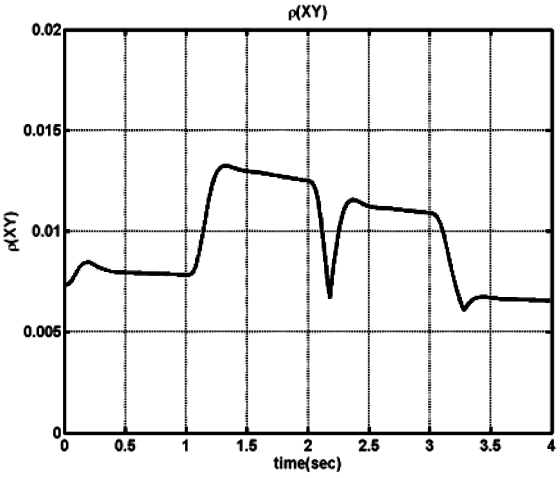

Fig. 9. Variation of $\rho(\hat{X}\hat{Y})$ with $\rho_c = 1.3$, $\gamma = 4$.

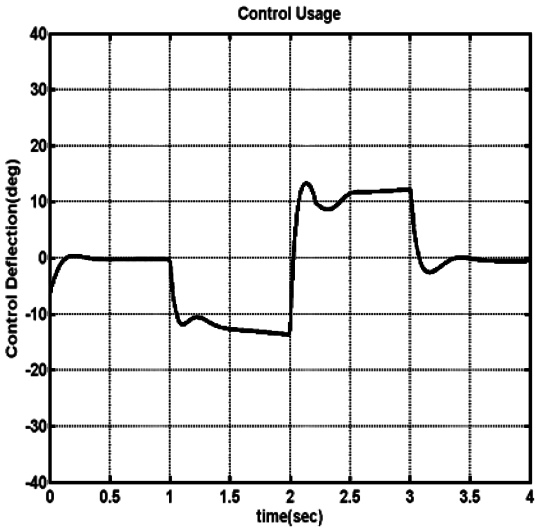

Fig. 11. Control usage with $\rho_c = 2$, $\gamma = 4$.

$Y(\hat{x}) > 0$ fail (see [14]). In order to show the effect of the control weight ρ_c, we set it to 2 and the results for this case are presented in Figs. 10–11. As can be seen, the maximum control usage is reduced but normal acceleration tracking is slower than the tracking with smaller ρ_c.

Figs. 12–14 demonstrate the tracking performance when γ is set to 3.65. As can be seen, the tracking performance degrades after about 2.5 s. This can be related very well to the history of $\rho[X(\hat{x})Y(\hat{x})]$ in Fig. 14. The condition $\rho[X(\hat{x})Y(\hat{x})] < \gamma^2$ is violated quickly after 2.5 s.

Since we are dealing with nonlinear systems, we expect to find a varying and tighter γ which will satisfy the three conditions of the H_∞ problem at each time. After we know a rough lower bound of γ as 4, we proceed to search for smaller γ when applying the $\theta - D$ H_∞ controller at each time. An iterative process is used at each epoch to find a γ starting from 4 such that the three conditions (i–iii) are satisfied. Figs. 15–16 show the results where γ is found to be further reduced to the range of $[0.05, 1]$. As observed from Fig. 15, tracking history is good and is not much different from Fig. 3. The only discernible difference occurs from 0.1 s to 0.2 s. Fig. 16 presents $\rho[X(\hat{x})Y(\hat{x})]$ history. They are all well behaved.

Another issue associated with this design is the parameter (k_1, l_1) and (k_2, l_2) in D_1 and D_2 matrices. They are chosen as $(1, -10)$ for both. These parameters are selected based upon many initial conditions of interest. For the initial state $x_0 = [2.5\ 0\ 0\ 0\ 0\ 0\ 0]^T$, the tracking is good and the control usage is reasonable even without D_1 and D_2. To demonstrate the function of D_1 and D_2, the results from a different initial state $x_0 = [3.5\ 5^\circ\ 5^\circ\ 10^\circ/s\ 0\ 0\ 0]^T$ are given in Figs. 17–20. As can be seen from Fig. 18, the initial maximum control is about 56° without D_1 and D_2 but is reduced to 24° with D_1 and D_2 added in Fig. 20. The selection of (k_i, l_i) in D_i terms is problem dependent. A large exponential parameter is chosen in this particular

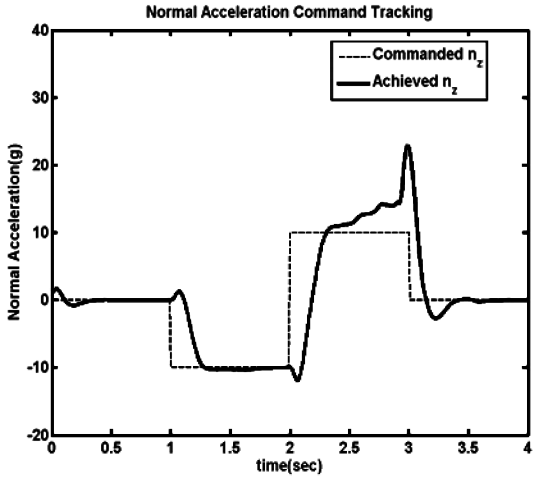

Fig. 12. Normal acceleration with $\rho_c = 1.3$, $\gamma = 3.65$.

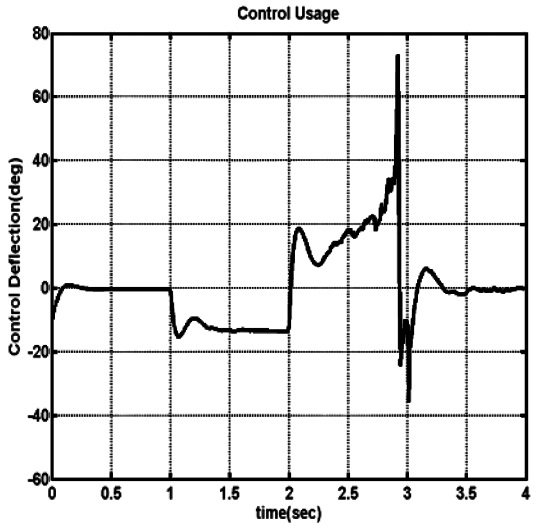

Fig. 13. Control usage with $\rho_c = 1.3$, $\gamma = 3.65$.

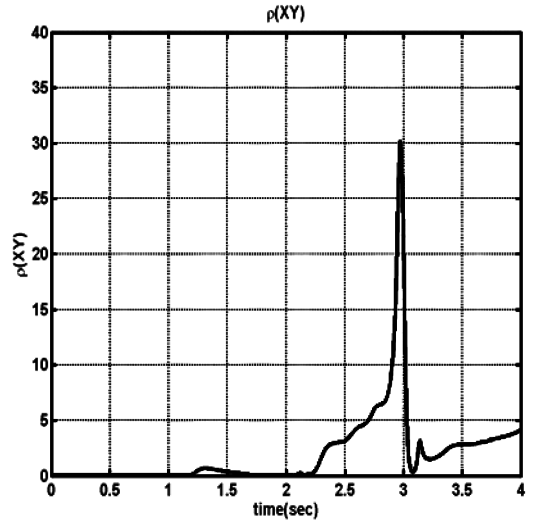

Fig. 14. Variation of $\rho(\hat{X}\hat{Y})$ with $\rho_c = 1.3$, $\gamma = 3.65$.

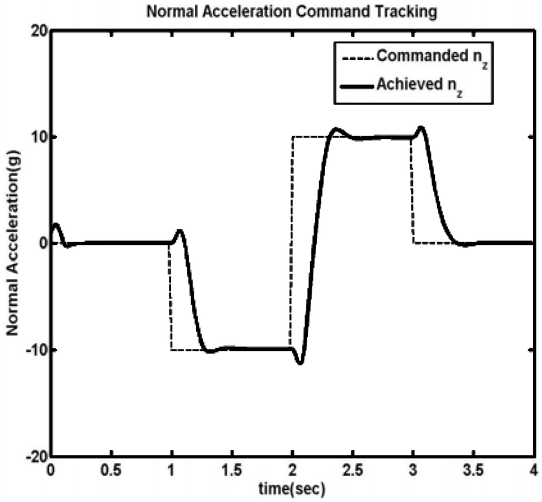

Fig. 15. Normal acceleration with varying γ.

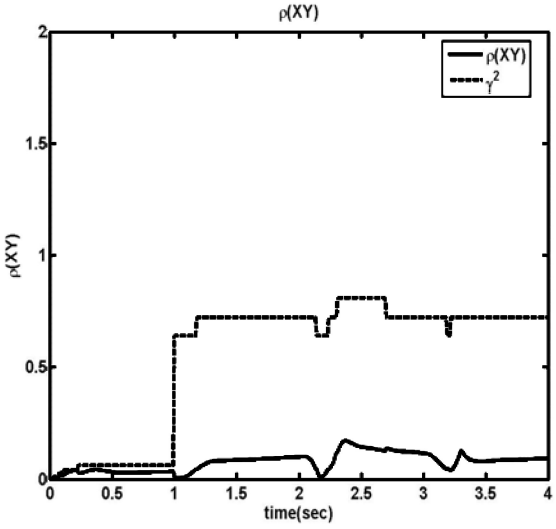

Fig. 16. Variation of $\rho(\hat{X}\hat{Y})$ with respect to varying γ.

problem because we found that the large control only happens at a very early stage. It may not be the case [12, 17] for other problems in which (k_i, l_i) could be small values. These are design parameters that need tuning.

To demonstrate the effectiveness of the nonlinear $\theta - D$ H_∞ design, a linear H_∞ design is employed on the linearized missile dynamics and is compared with the nonlinear $\theta - D$ H_∞ design. The linearization is performed by taking the Jacobian of $f(x)$ and $c_y(x)$ in (23) and (25), respectively

$$\dot{\tilde{x}} = \tilde{A}\tilde{x} + B_w w + B_u u \tag{81}$$

$$\tilde{z} = C_z \tilde{x} + D_{zu} u \tag{82}$$

$$\tilde{y} = \tilde{C}_y \tilde{x} + D_{yw} w \tag{83}$$

where

$$\tilde{x} = x - x_0, \qquad \tilde{A} = \left.\frac{\partial f(x)}{\partial x}\right|_{x_0}, \qquad \tilde{C}_y = \left.\frac{\partial c_y(x)}{\partial x}\right|_{x_0}$$

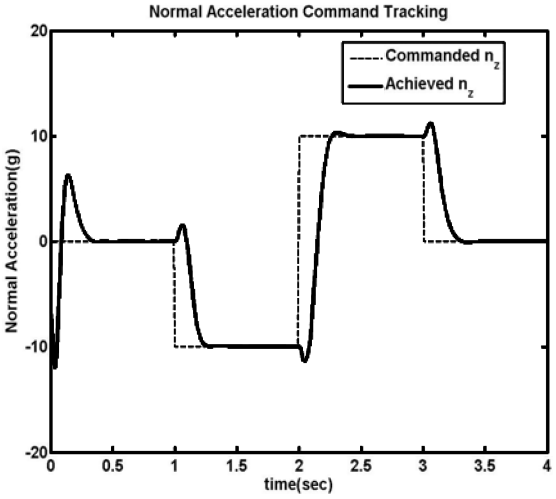

Fig. 17. Normal acceleration with $x_0 = [3.5\ 5^\circ\ 5^\circ\ 10^\circ/s\ 0\ 0\ 0]^T$ and $\rho_c = 1.3$ without D_i.

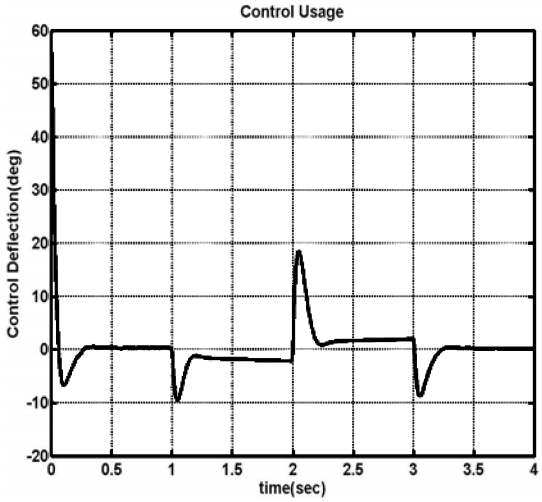

Fig. 18. Control usage with $x_0 = [3.5\ 5^\circ\ 5^\circ\ 10^\circ/s\ 0\ 0\ 0]^T$ and $\rho_c = 1.3$ without D_i.

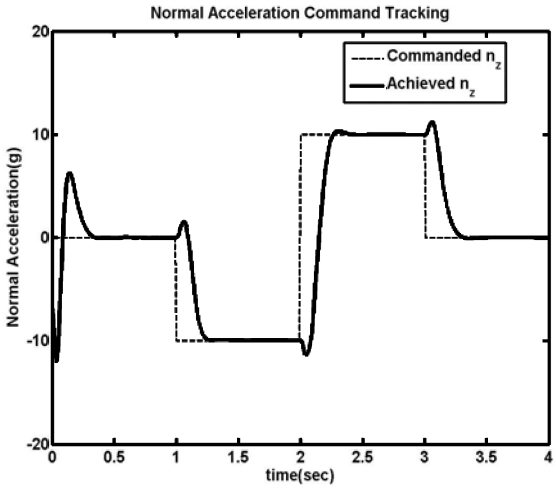

Fig. 19. Normal acceleration with $x_0 = [3.5\ 5^\circ\ 5^\circ\ 10^\circ/s\ 0\ 0\ 0]^T$ and $\rho_c = 1.3$ with D_i added.

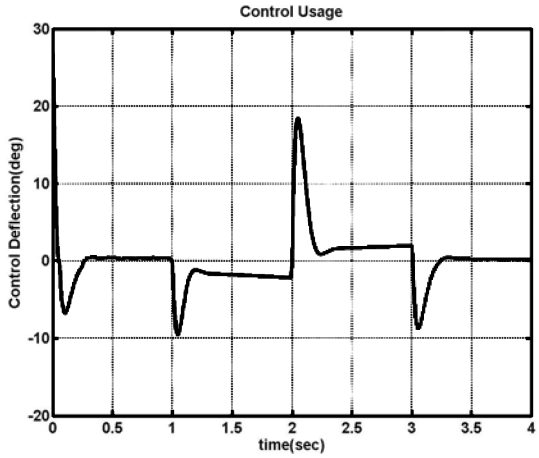

Fig. 20. Control usage with $x_0 = [3.5\ 5^\circ\ 5^\circ\ 10^\circ/s\ 0\ 0\ 0]^T$ and $\rho_c = 1.3$ with D_i added.

and x_0 is the operation point at which the linearization is taken. B_w, B_u, C_z, D_{zu}, and D_{yw} are constant matrices. The linear H_∞ controller is designed based upon the linearized model (81)–(83) and applied to the original nonlinear model. The simulation results are shown in Figs. 21–28. Figs. 21–26 demonstrate the results at the operating point $x_0 = [2.5,0,0,0,0,0,0]^T$ which is the same as the initial states. As can be seen, the tracking performance is only good during the first second. They do not work well after 1 s because the jump in the normal acceleration gives rise to large deviations of the states from the linearized point. The minimum γ in linear H_∞ design is 6.05. Note that the nonlinear $\theta - D$ H_∞ controller is designed with a constant $\gamma = 4$. Figs. 27–28 show the normal acceleration tracking and control usage when the operating point is chosen to be $x_0 = [2.5, -5^\circ, 5^\circ, -20^\circ/s, 0, 0, 0]^T$. It can be observed that the performance after 1 s is better than that at the first operating point. However, the normal acceleration history is worse during the first second and the maximum control usage goes up to 46°. The minimum γ in this case is 6.25. In comparison, the nonlinear $\theta - D$ H_∞ controller performs much better than the linear H_∞ controller at both operating points. In addition, the γ value of nonlinear H_∞ design is smaller than that of the linear H_∞ design.

As for implementation of the $\theta - D$ H_∞ controller, the major advantage the $\theta - D$ technique provides is a closed-form solution to the SDRE for the nonlinear H_∞ problem. Thus, evaluating the closed-form expression for $X(\hat{x})Y(\hat{x})$ obtained from the $\theta - D$ algorithm is much easier. Specifically, the $\theta - D$ algorithm needs only one matrix inverse operation off-line when solving the linear Lyapunov equations (49)–(51). When implemented online, this method involves only three 7×7 matrix multiplications and three 7×7 matrix additions if we take three terms in control. However, in comparison, SDRE

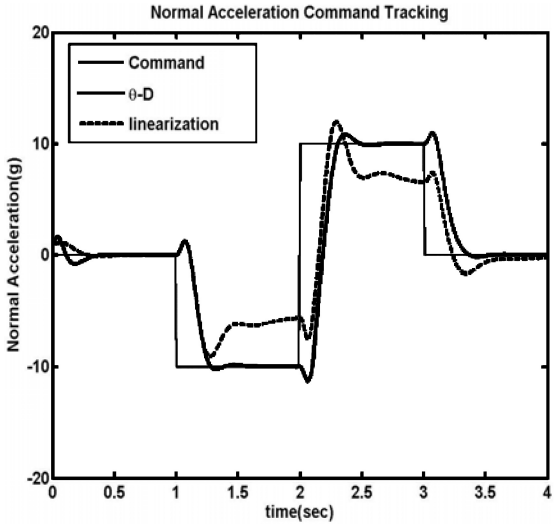

Fig. 21. Normal acceleration comparison.

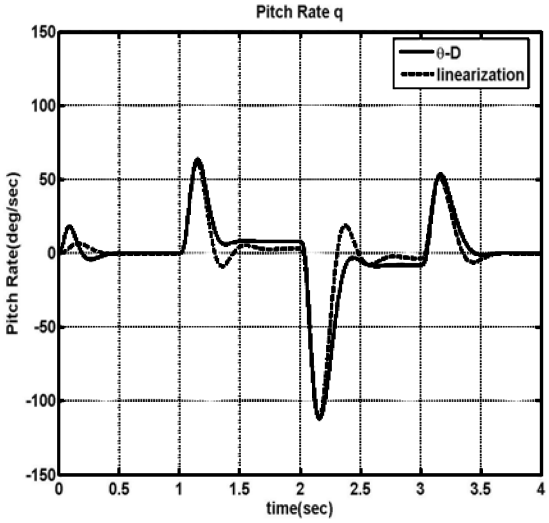

Fig. 24. Pitch rate comparison.

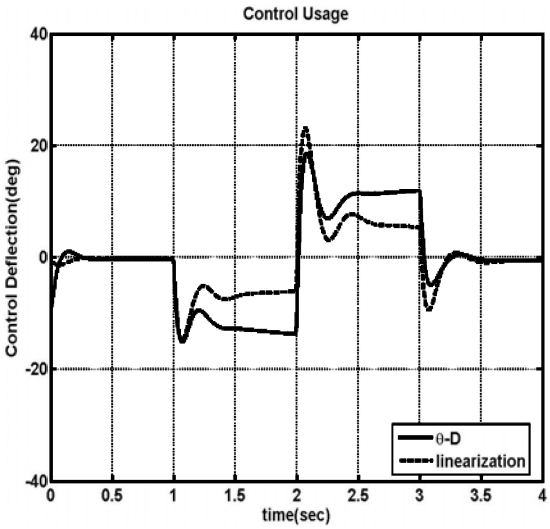

Fig. 22. Control usage comparison.

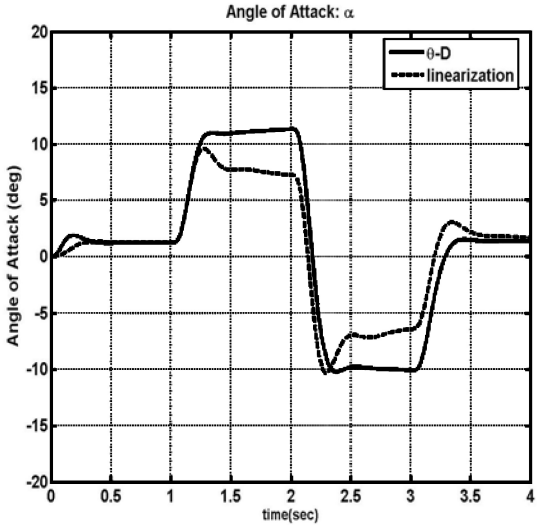

Fig. 25. Angle of attack comparison.

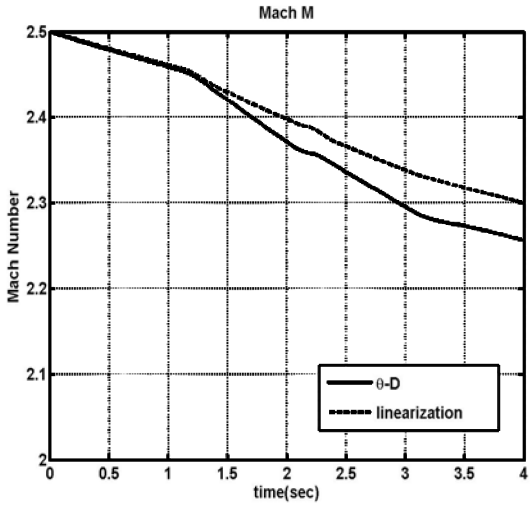

Fig. 23. Mach number comparison.

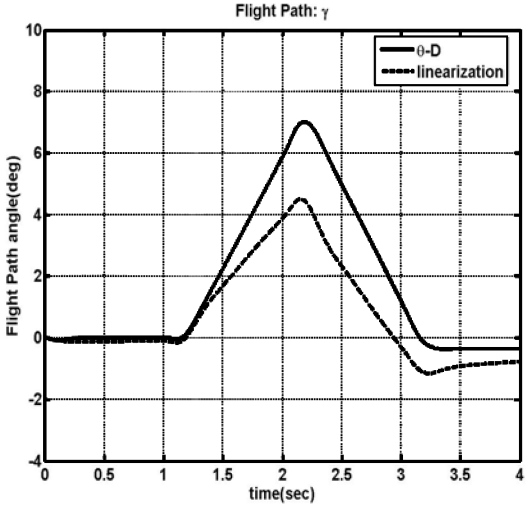

Fig. 26. Flight path angle comparison.

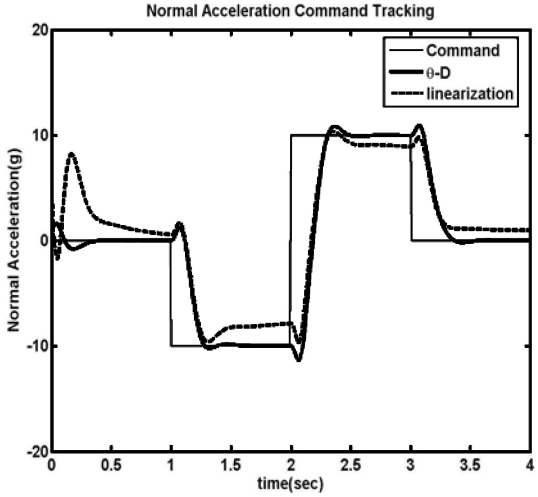

Fig. 27. Normal acceleration comparison at different operating point.

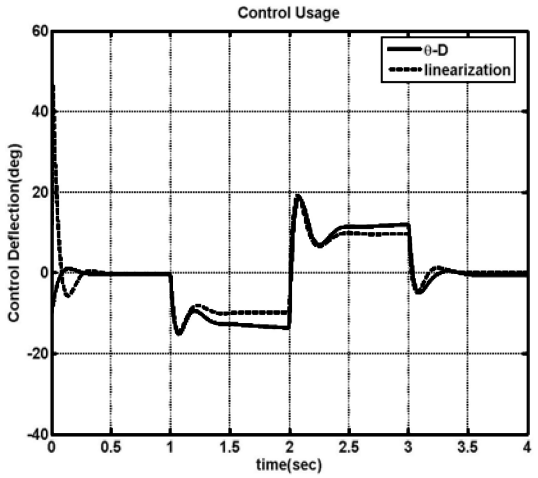

Fig. 28. Control usage comparison at different operating point.

needs computation of the 7×7 algebraic Riccati equation at each sample time which consumes much computational power. The number of computations will become more significant if we want to solve higher order problems with the SDRE method. For this nonlinear H_∞ control problem, one needs to check the condition $\rho[X(\hat{x})Y(\hat{x})] < \gamma^2$ at each state. If this condition was violated, γ needs to be raised accordingly. So to implement the SDRE technique, one needs to solve the state dependent Riccati equation at every instant plus check the eigenvalue condition. But for the $\theta - D$ method, the only thing that demands computational power is to check the eigenvalues of $X(\hat{x})Y(\hat{x})$. On the other hand, to avoid the computation of eigenvalue, one could select a large enough (lower bound) constant γ to ensure that the eigenvalue condition is valid for the whole state space. In [7], [18], a constant γ is adopted although the eigenvalue condition is not used. This design may be conservative. But the performance results in this study do not show much variation for a constant γ and a varying γ as can be seen from Figs. 3–8 and Figs. 15–16.

In the feedback controller design, it was assumed that the missile model described by (18)–(21) is accurate. In reality, this is not true due to the inevitable parameter uncertainties in the aerodynamic coefficients. There are many papers in literature that investigate robust H_∞ design in the presence of structured model uncertainties. For linear systems, some effective synthesis tools for robust linear H_∞ design such as μ synthesis [14] are available. However, for nonlinear systems, this is still an open area. Some analysis for the existence of the robust nonlinear H_∞ controller have been carried out and one can refer to [19], [20] and the references therein. However, there still exists the gap between the analysis and synthesis for the robust nonlinear H_∞ control problem. In this paper, we consider the standard nonlinear H_∞ control problem described by (23)–(25) without uncertainties. The objective of our nonlinear H_∞ controller synthesis is to achieve closed-loop stability and to attenuate the influence of the exogenous input w on the regulated variable z by γ. The major contribution of this paper is to provide a new solution to this nonlinear control problem. Robustness to the parameter uncertainties will form future research work and is beyond the scope of this paper. The $\theta - D$ H_∞ controller in this study does show robustness to the parameter variations. To study this, we perturbed the force coefficient C_Z and moment coefficient C_m in the missile model by $\pm 25\%$ in the simulations while using the controller based on the exact model similar to [2]. The results are shown in Figs. 29–30. As can be seen, the controller is still able to stabilize the system with acceptable performance. Other successful applications of the $\theta - D$ technique in the face of large parameter variations can be found in [12], [17].

VII. CONCLUSIONS

In this paper, a new suboptimal nonlinear H_∞ control technique was applied to the missile longitudinal autopilot design. Approximate closed-form solutions to the resulting SDREs in the nonlinear H_∞ formulation can be obtained by the $\theta - D$ method. Compared with an SDRE H_∞ design, this approach does not need intensive on-line computation of Riccati equation and thus is easy to implement. Performance comparison with a linearized H_∞ design has shown the potential of a nonlinear design. It should however be noted that as in the case of the SDRE solution, the three conditions for the existence of solutions of the H_∞ problem have to be evaluated on-line.

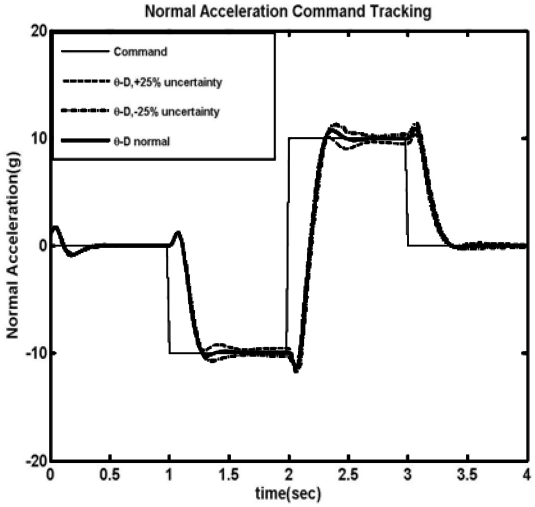

Fig. 29. Normal acceleration under ±25% parameter uncertainty.

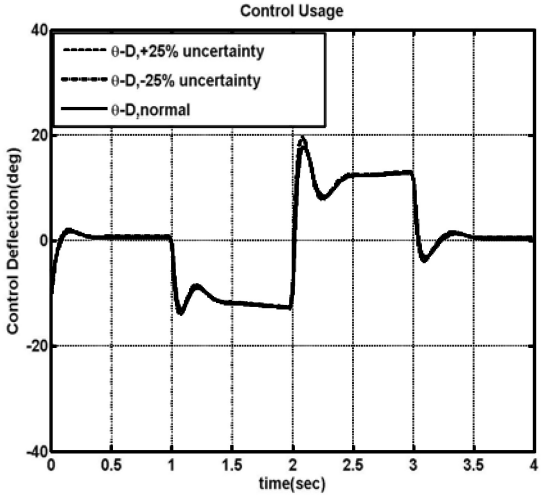

Fig. 30. Control history under ±25% parameter uncertainty.

REFERENCES

[1] Shamma, J. S., and Cloutier, J. R.
Gain scheduled missile autopilot design using linear parameter varying transformation.
Journal of Guidance, Control, and Dynamics, **16**, 2 (1993), 256–263.

[2] Nichols, R. A., Reichert, R. T., and Rugh, W. J.
Gain scheduling for H_∞ controllers: A flight control example.
IEEE Transactions on Control Systems Technology, **1**, 2 (1993), 69–78.

[3] Wu, F., Packard, A., and Balas, G.
LPV control design for pitch axis missile autopilots.
Presented at the 34th IEEE Conference on Decision and Control, Piscataway, NJ, 1995.

[4] Garrard, W. L.
Design of Nonlinear automatic flight control systems.
Automatica, **13** (1977), 497–505.

[5] Garrard, W. L., Enns, D. F. and Snell, S. A.
Nonlinear feedback control of highly manoeuverable aircraft.
International Journal of Control, **56** (1992), 799–812.

[6] McLain, T. W., and Beard, R. W.
Nonlinear optimal control design of a missile autopilot.
Presented at the AIAA Guidance, Navigation and Control Conference, Boston, MA, 1998.

[7] Wise, K. A., and Sedwick J. L.
Nonlinear H_∞ optimal control for agile missiles.
Journal of Guidance, Control and Dynamics, **19**, 1 (1996), 157–165.

[8] Cloutier, J. R., D'Souza, C. N., and Mracek, C. P.
Nonlinear regulation and nonlinear H_∞ control via the state-dependent Riccati equation technique.
Proceedings of the 1st International Conference on Nonlinear Problems in Aviation and Aerospace, vol. 1, Reston, VA, 1996, 117–123.

[9] Mracek, C. P., and Cloutier, J. R.
State dependent Riccati equation techniques: Theory and applications.
Presented at the IEEE American Control Conference Workshops, June 23, 1998.

[10] Palumbo, N. F., and Jackson, T. D.
Integrated missile guidance and control: A state dependent Riccati differential equation approach.
Proceedings of the 1999 IEEE International Conference on Control Applications, Hawaii, Aug. 22–27, 1999.

[11] Xin, M., and Balakrishnan, S. N.
Missile longitudinal autopilot design using a new suboptimal nonlinear control method.
IEE Proceedings on Control Theory and Applications, vol. 150, 2003, 577–584.

[12] Xin, M., Balakrishnan, S. N., Stansbery, D. T., and Ohlmeyer, E. J.
Nonlinear missile autopilot design with theta-D technique.
AIAA Journal of Guidance, Control and Dynamics, **27**, 3 (2004), 406–417.

[13] Mracek, C. P., and Cloutier, J. R.
Missile longitudinal autopilot design using the state dependent Riccati equation method.
Proceedings of the First International Conference on Nonlinear Problems in Aviation and Aerospace, Daytona Beach, FL, May, 1996.

[14] Zhou, K., and Doyle, J. C.
Essentials of Robust Control.
Upper Saddle River, NJ: Prentice-Hall, 1998.

[15] Xin, M.
A new method for suboptimal control of a class of nonlinear systems.
Optimal Control Applications and Methods, **26**, 2 (2005), 55–83.

[16] Bryson, A. E., Jr., and Ho, Y.-C.
Applied Optimal Control.
Washington, DC: Hemisphere Publishing, 1975.

[17] Drake, D., Xin, M., and Balakrishnan, S. N.
A new nonlinear control technique for ascent phase of reusable launch vehicles.
AIAA Journal of Guidance, Control and Dynamics, **27**, 6 (2004), 938–948.

[18] Yang, C. D., and Kung, C. C.
Nonlinear H_∞ flight control of general six-degree-of-freedom motions.
AIAA Journal of Guidance, Control and Dynamics, **23**, 2 (2000), 278–288.

[19] Lu, G., Zheng, Y., and Ho. D. W.
Nonlinear robust H_∞ control via dynamic output feedback.
Systems & Control Letters, **39**, 3 (2000), 193–202.

[20] Nguang, S. K.
Robust nonlinear H_∞ output feedback control.
IEEE Transactions on Automatic Control, **41**, 7 (1996), 1003–1007.

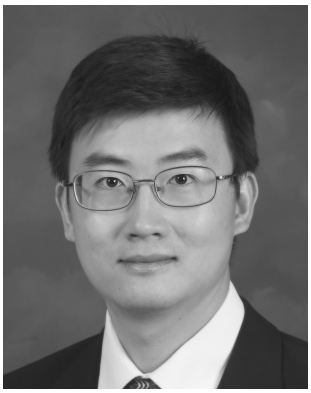

Ming Xin (M'02) received the B.E. and M.E. degrees in automatic control from the Nanjing University of Aeronautics and Astronautics, Nanjing, China, in 1993 and 1996, respectively, and the Ph.D. degree in aerospace engineering from the University of Missouri–Rolla, Rolla, in 2002.

He worked as a postdoctoral research fellow at University of Missouri–Rolla since 2003. He is currently an assistant professor with the Department of Aerospace Engineering at the Mississippi State University, Starkville. His research interests include nonlinear control theory, guidance and control of aerospace vehicles, multiple vehicle dynamics and control, neural networks, and estimation.

Dr. Xin is a member of the American Institute of Aeronautics and Astronautics (AIAA).

S. N. Balakrishnan received the Ph.D. degree in aerospace engineering from the University of Texas at Austin, Austin.

He has been with the University of Missouri–Rolla, Rolla, since 1985. Currently, he is a professor with the Department of Mechanical and Aerospace Engineering. His nonteaching experience includes work as a lead engineer in the Space Shuttle program, Fellow, Center for Space Research at the University of Texas at Austin, summer Faculty Fellow at Air Force Research Laboratory, Eglin, FL, and engineer, Indian Space Program. His research interests include areas of system theory and applications. His current research uses neural networks and classical methods in the identification and robust control of missiles, airplanes, rockets, and other "interesting" systems. His research has been sponsored by the National Science Foundation (NSF), the Air Force, the Naval Surface Warfare Center, the Army Space and Missile Defense Command, and NASA.

Dr. Balakrishnan is a member of Sigma Gamma Tau. He is an Associate Fellow of the American Institute of Aeronautics and Astronautics (AIAA).